Journal of Applied Polymer Science

Synthesis and Characterization of Novel Phosphorous-Silicone-Nitrogen Flame Retardant and Evaluation of Its Flame Retardancy for Epoxy Thermosets

Zhi-Sheng Li, Jin-Gang Liu, Tao Song, Deng-Xiong Shen, Shi-Yong Yang
Laboratory of Advanced Polymer Materials, Institute of Chemistry, Chinese Academy of Sciences, Beijing 100190, China
Correspondence to: J.-G. Liu (E-mail: liujg@iccas.ac.cn) or S.-Y. Yang (shiyang@iccas.ac.cn)

ABSTRACT: A novel phosphorous-silicone-nitrogen ternary flame retardant (FR), [(1,1,3,3-tetramethyl-1,3-disilazanediyl)di-2,1-ethanediyl]bis(diphenylphosphine oxide) (PSiN) was synthesized with high yield via a one-step procedure by the reaction of diphenylphosphine oxide and vinyl-terminated silazane with triethylborane as the catalyst. The chemical structure of the target compound was confirmed by nuclear magnetic resonances, matrix-assisted laser desorption/ionization time-of-flight mass spectrometry, and Flourier transform infrared measurements. The developed PSiN FR was applied in the flame retardancy of *o*-cresol novolac epoxy (CNE)/phenolic novolac (PN) hardener system. Effects of PSiN on the processability, thermal properties, especially the flame retardancy properties of the composites were investigated. Experimental results revealed that addition of PSiN improved the flowability of the CNE/PN systems, while the thermal stability of the epoxy thermosets was maintained. Meanwhile, the incorporation of PSiN was in favor of the formation of char during the thermal degradation process of the epoxy thermosets. The limited oxygen index of the epoxy system increased along with the PSiN content. An UL 94 V-0 FR rating was achieved when the weight content of PSiN in the epoxy composites reached 20 wt %. © 2014 Wiley Periodicals, Inc. J. Appl. Polym. Sci. **2014**, *131*, 40412.

KEYWORDS: flame retardance; resins; thermosets

Received 22 August 2013; accepted 9 January 2014
DOI: 10.1002/app.40412

INTRODUCTION

Flame retardancy has been becoming an ever-increasingly important issue for applications of general engineering polymers.[1,2] For instance, epoxy resins are widely used as encapsulating materials for integrated circuit components due to their excellent combined properties, including good thermal, mechanical, and dielectric properties and at the same time, a relatively low cost.[3,4] Demands for flame retardancy are extremely strong for these epoxy resins in consideration that they are commonly inflammable in nature and often exposed to high-temperature environments during their service.[4] In the flame retardancy research field for epoxy resins, much attention has been paid to the design and development of novel flame retardants (FRs) with high efficiency, good environmental compatibility, and low cost in recent years.[2]

Between the two common types of FRs for epoxy systems, organic FRs usually exhibit excellent comprehensive properties, such as high FR efficiency, good compatibility with epoxy matrix, and outstanding flexibility for their molecular designs compared with their inorganic counterparts. For instance, in advanced thin-type microelectronic packaging, conventional epoxy encapsulating materials with inorganic metal hydroxide (magnesium hydroxide or aluminum hydroxide) as FRs are facing increasing challenges due to the negative effects of moldability and curability of the epoxy systems caused by the high loading levels (low efficiency) of the inorganic FRs.[5] Alternatively, organic FRs can usually achieve a good balance among the flowability, moldability, curability, and reliability for epoxy systems.[6]

Among various organic FRs, the species containing phosphorus elements have been extensively used in epoxy flame retardancy applications.[7,8] The phosphorus-based compounds can act as FRs in both gas and condensed phase depending on their chemical structures[9]; thus have been widely employed for epoxy flame retardancy. For example, 9,10-dihydro-9-oxa-10-phosphaphenanthrene-10-oxide (DOPO), a phosphorus-containing heterocyclic compound, has attracted intensive attention due to its high flame retarded efficiency and active reactivity. Various epoxy resins, curing agents, and additives based on DOPO have been prepared and reported intensively.[10–14] Diphenylphosphine oxide (DPPO) is another important phosphorus-containing compound, which has a similar chemical structure with DOPO. However, it has been revealed that the P—C bonds in DPPO

usually exhibit a superior hydrolysis resistance than that of P—O—C bonds in DOPO.[9,15,16] This is important for epoxy thermosets used in electronic applications. Epoxy resin based on the bisphenol derived from DPPO and *p*-benzoquinone, that is (2,5-dihydroxyphenyl)-diphenylphosphine oxide has been developed and cured with 4,4′-diaminodiphenylmethane.[17] Higher glass transition temperatures (T_g) and limiting oxygen index (LOI) values are achieved for the DPPO-containing epoxy systems compared with the common diglycidyl ether of bisphenol A (DGEBA) thermoset. It can be anticipated that the FRs containing DPPO moiety might exhibit excellently comprehensive properties. However, to the best of our knowledge, there are few reports in existing literature on DPPO-based FRs.

In the present work, a novel FR containing DPPO moiety in its structure has been designed and synthesized. In addition, nitrogen and silicon elements are also introduced into the FR. This molecular design is mainly based on our previous study, in which a series of P-Si FRs were developed.[18] Nitrogen-containing FRs usually produce incombustible gases in combustion, which can efficiently dilute the concentration of the oxygen around the flame.[19,20] While silicon-containing FRs are considered to be one of the "environmentally friendly" and highly efficient flame retardant materials.[21–23] Thus, the current P-Si-N ternary FR might exhibit good FR efficiency for common polymers. In this article, a novel P-Si-N FR, [(1,1,3,3-tetramethyl-1,3-disilazanediyl)di-2,1-ethanediyl]bis(diphenylphosphine oxide) (PSiN) was first synthesized. Then, the FR was applied in a typical *o*-cresol novolac epoxy (CNE)/phenolic novolac (PN) hardener system. The effects of PSiN on various properties of the epoxy systems, including processability, curability, thermal stability, and FR properties were investigated in detail. Atlast, the primary FR mechanism of PSiN in the epoxy thermoset was studied.

EXPERIMENTAL

Materials

Triethylborane (1.0 mol L^{-1} solution in hexane) was purchased from Sigma-Aldrich and used as received. 1,3-Divinyl-1,1,3,3-tetramethyldisilazane (DVTMDZ) was purchased from Alfa-Aesar and distilled prior to use. DPPO was bought from Beijing POME Sci. Technol. Co. Ltd., China and purified by recrystallization from toluene before use. PN (TD-2131, a product of Dainippon Ink & Chemicals Inc., Japan; hydroxyl equivalent: 105 g mol^{-1}; softening point: 80°C) and CNE (195LL, a product of Nippon Kayaku Co., Japan; epoxy equivalent: 195 g mol^{-1}; softening point: 70°C) were purchased and used as supplied. Triphenylphosphine (TPP) was bought from Beijing Chemical Reagent Company, China and used without purification. All the other commercially available reagents were used as received. Chemical structures of CNE, PN, and TPP are shown in Figure 1(a).

Characterization

Fourier transform infrared (FTIR) spectra were recorded on a Perkin–Elmer 2000 FTIR spectrometer. Nuclear magnetic resonance spectra (^{1}H-NMR and ^{13}C-NMR) were conducted on a Bruker AV-400 nuclear magnetic resonance spectrometer with tetramethylsilane as the internal standard. ^{29}Si-NMR and ^{31}P-NMR measurements were performed on a Bruker DMX 300 spectrometer. Matrix-assisted laser desorption/ionization time-of-flight mass spectrometry (MALDI-TOF-MS) spectra were obtained on a Biflex III mass spectrometer. Differential scanning calorimeter (DSC) measurements were performed with a TA Instruments Q100 DSC with standard aluminum pans. Rheological measurements for the compacted resin discs were performed using a parallel-plate fixture (diameter: 25 mm, gap 2.0 mm) by an oscillation mode with a shear rate of 10 rad s^{-1} and a heating rate of 4 °C min^{-1}. Thermogravimetric analysis (TGA) measurements were performed with a TA Instruments Q50 at a heating rate of 20 °C min^{-1}. *In situ* FTIR (or real-time FTIR) spectra were recorded with a Nicolet 8700 spectrometer (Nicolet Instrument Co., USA). The KBr method was used for measuring the *in situ* FTIR spectra in the range from room temperature to 500°C at a heating rate of 10 °C min^{-1}. Flame retardancy of the thermal-cured resins was determined by the LOI method specified in ASTM D289. The forced-flaming behavior of the cured products was investigated using a cone calorimeter following ASTM E1354. UL 94 test was also used to evaluate the flame retardancy, which was performed using sheets (100 mm × 13.0 mm × 3.0 mm) according to ASTM D635-77. The morphology of the samples was observed with a scanning electronic microscope (SEM, Hitachi S-4300, Japan). Energy dispersive X-ray (EDX) measurements were conducted with EX-350 micro analyzer equipped in the SEM. X-ray photoelectron spectroscopy (XPS) data were obtained with an ESCALab220i-XL electron spectrometer from VG Scientific using a 300 W MgKα radiation. The base pressure was 3 × 10^{-9} mbar. The binding energies were referenced to the C1s line at 284.8 eV from the adventitious carbon.

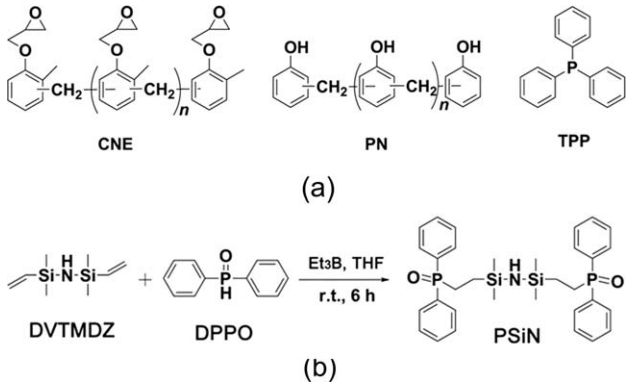

Figure 1. (a) Typical molecular structures of chemicals used in the study, (b) synthesis of FR PSiN.

Synthesis of PSiN

The FR PSiN was synthesized with a procedure as shown in Figure 1(b). DPPO (40.4 g, 0.2 mol), DVTMDZ (18.5 g, 0.1 mol), and tetrahydrofuran (500 mL) were added into a 1,000-mL three-necked round-bottom flask equipped with a stirrer, a nitrogen inlet, and a dropping funnel. The mixture was stirred at room temperature in nitrogen until all of the reactants dissolved. A stoichiometric triethylborane solution in hexane (100 mL, 0.1 mol) was added dropwise. After the addition, the progress of the reaction was monitored by thin layer chromatography (TLC). After the reaction was judged complete (usually after 5–6 h) by TLC, the reaction mixture was evaporated to

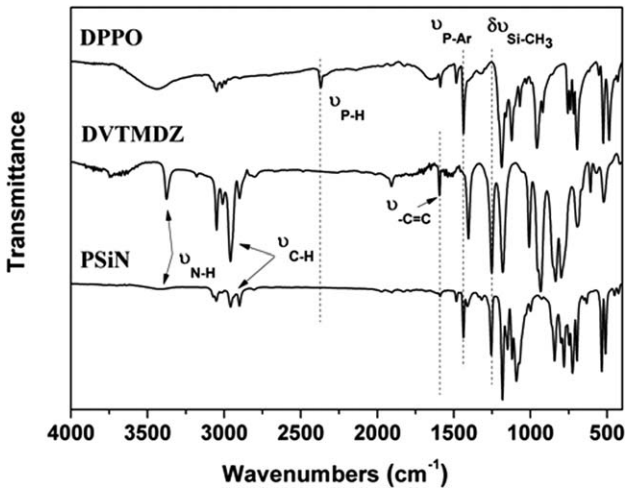

Figure 2. FTIR spectra of DPPO, DVTMDZ, and PSiN.

remove the tetrahydrofuran. The resulting solid was successively washed by diethyl ether and distilled water for three times. Then, the white solid was further purified by recrystallization from tetrahydrofuran to afford PSiN (51.6 g) with a yield of 88%.

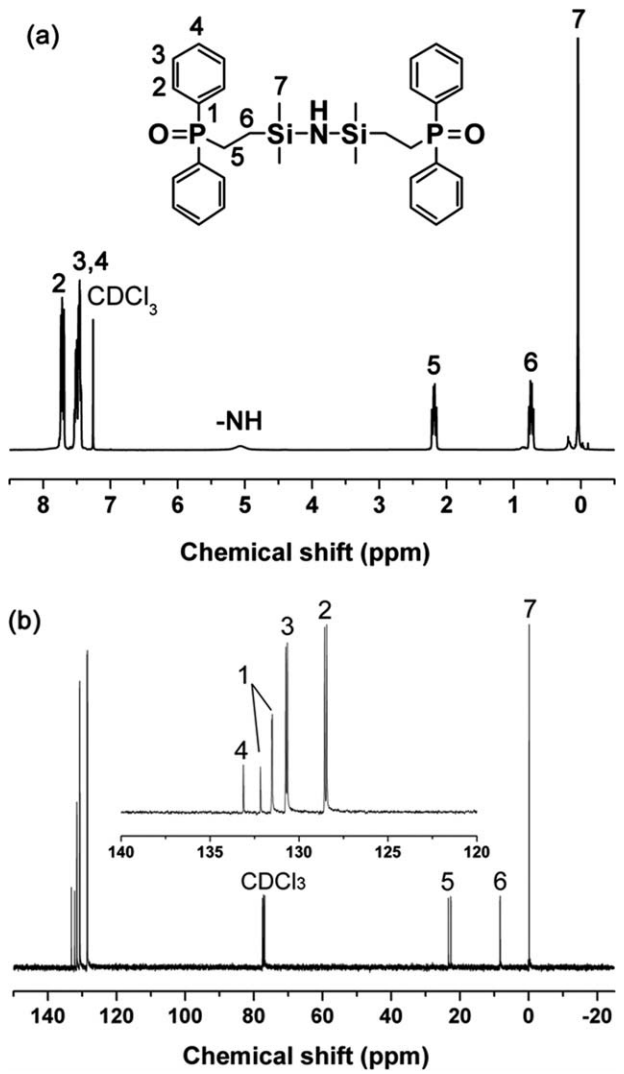

Figure 3. NMR spectra of PSiN. (a) ^{1}H-NMR and (b) ^{13}C-NMR.

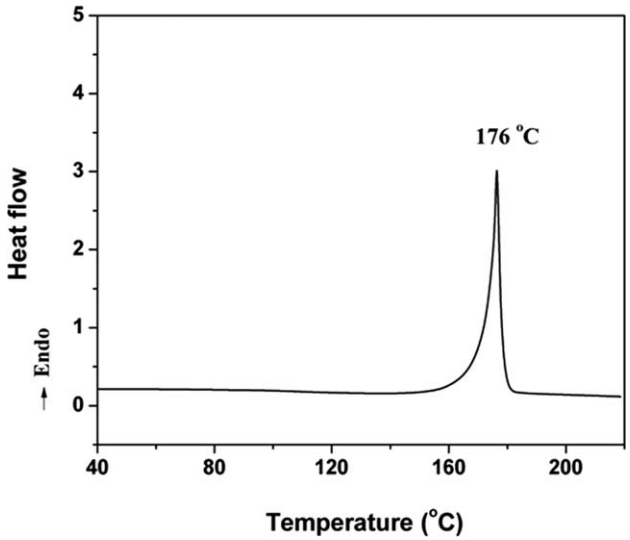

Figure 4. DSC curves of PSiN at a heating rate of 10 °C min^{-1}.

Melting point: 176°C (DSC peak temperature). FTIR (KBr, cm^{-1}): 3416 (N—H), 3051, 2958, 2900 (C—H), 1438 (P—Ar), 1256 (—$SiCH_3$), 1183 (P═O, Si—N), 800 (Si—C); ^{1}H-NMR (400 MHz, $CDCl_3$, δ ppm): −0.08(*s*, 12H, —Si—CH_3), 0.63 (*m*, 4H, —Si—CH_2—), 2.05 (*m*, 4H, —CH_2—P), 5.07 (*s*, 1H, —NH—), 7.30 (*m*, 12H, Ar—H), 7.60 (*m*, 8H, Ar—H); ^{13}C-NMR (101 MHz, $CDCl_3$, δ ppm): −0.19, 8.31, 23.3, 128.5, 130.7, 131.5, and 132.2; ^{29}Si NMR (60 MHz, $CDCl_3$, δ ppm): 11.8; ^{31}P-NMR (162 MHz, $CDCl_3$, δ ppm): 34.41; MALDI-TOF-MS, *m/z* : calcd. for $C_{32}H_{41}O_2NP_2Si_2$ $[M+Na]^+$: 612.2, found: 612.2.

Preparation of the Epoxy Thermosets with PSiN

The flame retardant epoxy systems were prepared according to the resin chemical compositions. Stoichiometric CNE epoxy was blended with PN at 160°C under nitrogen with a molar ratio of 1.0/1.0 for epoxy groups to phenolic hydroxyl. Various amounts of PSiN (10 wt % for CNE/PN-10 and 20 wt % for CNE/PN-20)

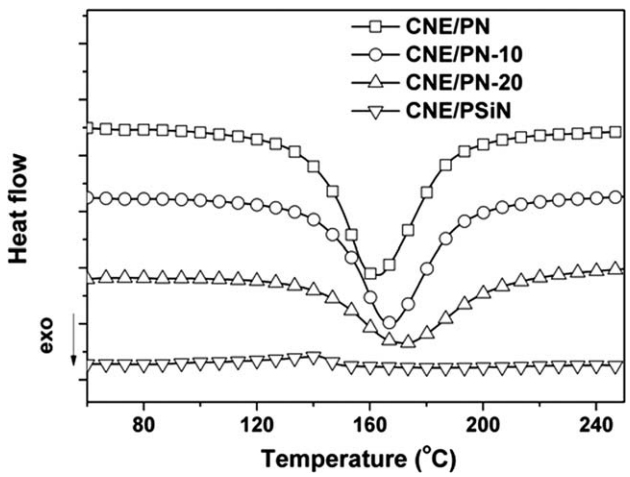

Figure 5. DSC curing curves of samples at a heating rate of 10 °C min^{-1}.

were then added. The mixture was stirred to give a homogeneous solution. Then, the mixture was cooled to 120°C, and TPP (1 wt % of CNE) was put in with mechanically stirring to ensure the catalyst well dispersed in the resin system. The well mixed epoxy resins were then cast into the pre-heated molds and thermally cured at 150°C for 3 h, followed at 180°C for 6 h. After post cured at 220°C for 3 h, cured epoxy thermosets, including CNE/PN, CNE/PN-10, and CNE/PN-20 were obtained.

RESULTS AND DISCUSSION

Flame Retardant PSiN Synthesis

The P-Si-N ternary FR PSiN was synthesized through a one-pot procedure using DPPO and DVTMDZ as the starting materials. This procedure has been proven to be an efficient pathway for the formation of P—C bonds.[24] In our experiments, the triethylborane catalyzed radical addition of DPPO to vinyl-silazane proceeded smoothly at room temperature affording PSiN with a high yield of 88%. The synthesized compound was characterized with FTIR, ^{1}H-NMR, ^{13}C-NMR, ^{31}P-NMR, ^{29}Si-NMR, DSC, and MODI-TOF measurements. Figure 2 shows the FTIR spectra of DPPO, DVTMDZ, and PSiN. It can be observed that the characteristic stretching vibration of P—H bond at 2377 cm^{-1} in DPPO and —C═C bond (in vinyl groups) at 1594 cm^{-1} in DVTMDZ all disappears completely in the spectrum of PSiN. While, the absorptions of N—H and C—H (in methyl groups) bonds in DVTMDZ are maintained in the spectrum of PSiN. The appearance of —$SiCH_3$ deformation vibration peak (1256 cm^{-1}) and P—Ar characteristic absorptions peak (1438 cm^{-1}) in PSiN confirms the successful preparation of the target compound.

The ^{1}H-NMR and ^{13}C-NMR spectra of PSiN are shown in Figure 3. In the ^{1}H-NMR spectrum [Figure 3(a)], the chemical shifts from 7.8 to 7.3 ppm (H_2, H_3, and H_4) are attributed to the protons in benzene ring, while the chemical shifts of —CH_2— (H_5 and H_6) can be found at 2–2.5 ppm and 0.5–1 ppm, respectively. Protons in methyl (H_7) attached to the silicon atom exhibit absorption in the farthest upfield region in the spectrum (~0 ppm). In addition, the signal at 5.1 ppm is assigned to the proton in the secondary amine group. The ^{13}C-NMR spectrum [Figure 3(b)] of PSiN reveals seven signals, which agrees with the predicated structure of PSiN. In the spectrum, C_1, C_2, and C_3 showed clear split doublet absorptions due to the coupling effects of carbons with the electron-withdrawing phosphine oxide groups in PSiN. This coupling effect decreased with the increase of the distance between C and P atoms, which can be deduced from the coupling constants. For instance, the coupling constants for C_1—P, C_2—P, and C_3—P are 68.7 MHz, 11.1 MHz, and 10.1 MHz, respectively. At last, the ^{31}P-NMR, ^{29}Si-NMR, DSC (shown in Figure 4) and MODI-TOF results also support the successful preparation of high-purity PSiN compound.

Curing Behavior of Epoxy/Curing Hardener/FR System

PSiN was mixed with CNE/PN with TPP as the curing accelerator to afford a series of epoxy thermosets. In order to figure out that whether PSiN get involved in the curing reaction of CNE/PN, we only added PSiN in the epoxy matrix without adding any other curing agents. Then, the epoxy systems were cured at elevated temperature. The curing reaction of the system was monitored by DSC and FTIR measurements, and the results are shown in Figures 5 and 6. No exothermic peak was detected in DSC heating curves. Besides, after the same cure procedure as CNE/PN, characteristic absorption peaks of epoxy groups (910 cm^{-1} and 844 cm^{-1}) still existed in the FTIR spectrogram. These results indicate that PSiN used in this work act as additive-type FR. We think that this is mainly due to the shielding effects of adjacent multi methyl substituents on the —NH— group. The curing behaviors of CNE/PN systems with different contents of PSiN were studied with DSC and rheometer measurements. Figure 5 shows the DSC curves for the curing procedure of epoxy systems (CNE/PN, CNE/PN-10, and CNE/PN-20) at a heating rate of 10 °C min^{-1}. The peak temperatures (T_p) are presented in Table I. It could be seen that the T_p values increased from 159°C to 172°C when the contents of PSiN ranged from 0 to 20 wt %, indicating that addition of PSiN in the epoxy systems retarded their curability to some extent. At the same time, the enthalpy values dropped from 262 J g^{-1} for CNE/PN to 225, 162 J g^{-1} for CNE/PN-10 and CNE/PN-20, respectively. The reasons for the decreases of the enthalpy values in the curing process are mainly attributed to two aspects. On one hand, PSiN has dilute effect on the CNE/PN blends. On the other hand, the addition of PSiN hinders the crosslinking reaction between CNE and PN.[5,8]

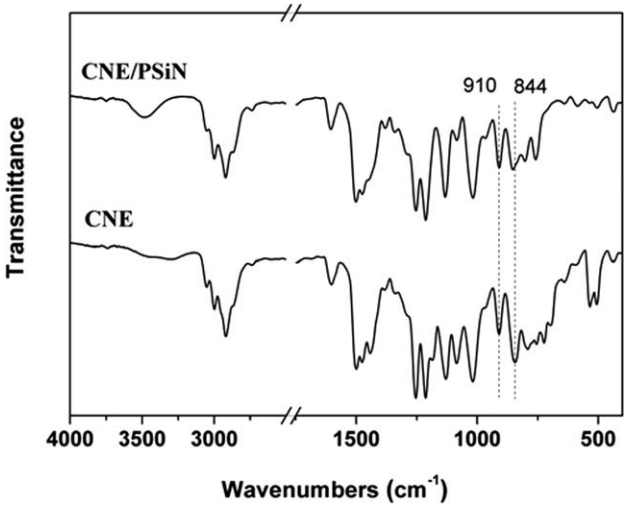

Figure 6. FTIR spectra of CNE and CNE/PSiN.

In order to investigate the effects of PSiN on the melting flowability of the epoxy systems, rheological tests of CNE/PN

Table I. Influence of PSiN on the Cure Process of CNE/PN

Samples	T_p [a](°C)	ΔH (J g^{-1})	η_{min} [b](Pa s)	T_{gel} [c](°C)
CNE/PN	159	266	8.5	137
CNE/PN-10	168	225	2.2	145
CNE/PN-20	172	162	2.3	147

[a] T_p, peak temperatures measured in DSC.
[b] η_{min}, minimum viscosities measured in rheological tests.
[c] T_{gel}, gel temperatures measured in rheological tests.

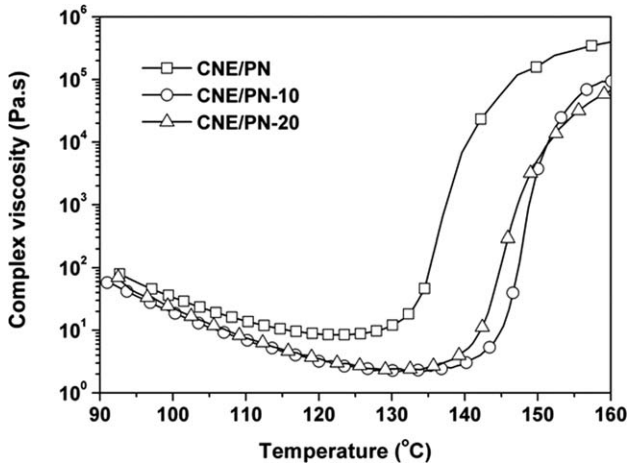

Figure 7. Rheology curves of samples at a heating rate of 4 °C min^{-1}.

systems were performed under oscillation mode at a heating rate of 4 °C min^{-1}. Figure 7 displays the rheological curves of CNE/PN systems. At first, the viscosities of these three samples all decreased along with the increasing temperatures due to the molecular chain movements in their structures. After that, the viscosities increased dramatically with increasing temperatures because of the occurrence of crosslinking. PSiN is a kind of chemical compound with small molecular weight, whose addition into the high-molecular-weight CNE/PN might act as a diluting agent. Thus, the viscosities of CNE/PN-10 and CNE/PN-20 are lower than that of CNE/PN material at a relatively low temperature. Moreover, with the incorporation of PSiN, the minimum viscosity (η_{min}, in Table I) decreases from 8.5 Pa s for CNE/PN to 2.2 Pa s for CNE/PN-10, and 2.3 Pa s for CNE/PN-20, respectively. The gel temperatures (T_{gel}) of the epoxy systems are determined as the intersection point of dynamical storage elastic modulus and loss elastic modulus in the rheological measurements. From the data in Table I, we could find that the T_{gel} values of the systems increased with the addition of PSiN. The drop of η_{min} values along with the rise of T_{gel} values indicates that the incorporation of PSiN can efficiently retard

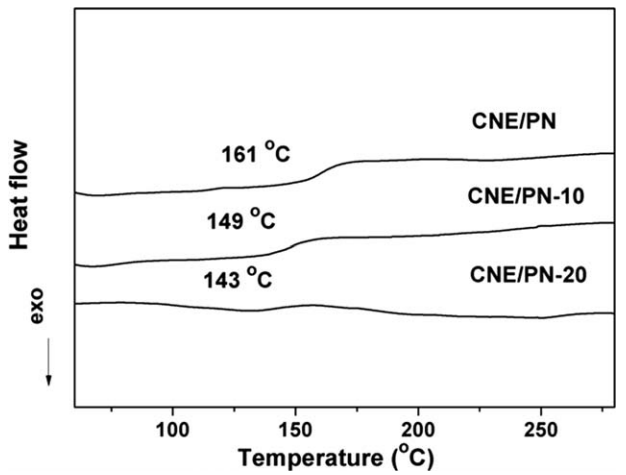

Figure 8. DSC curves of cured samples at a heating rate of 20 °C min^{-1}.

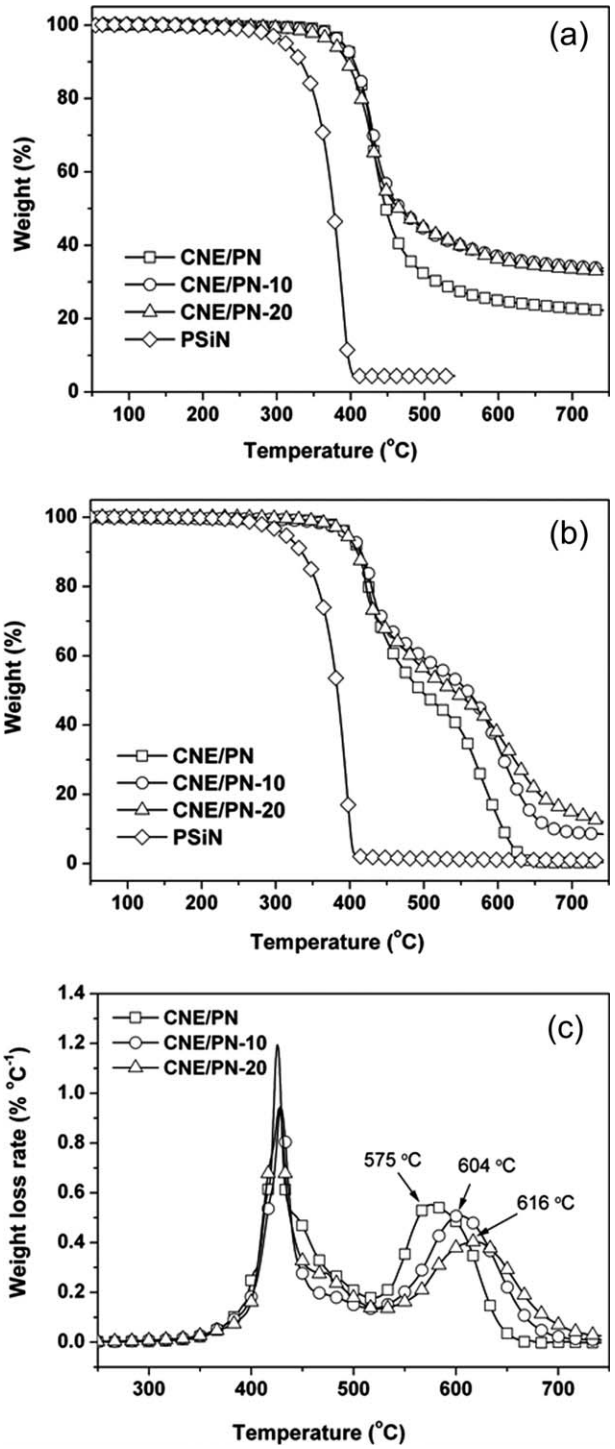

Figure 9. TGA curves of PSiN and the cured samples (a) in nitrogen; (b) in air; (c) DTGA in air.

the crosslinking reactions of CNE/PN systems. All these results reveal that the incorporation of PSiN can improve the flowability and processability of the CNE/PN systems, which is beneficial for their applications in microelectronic packaging.

Thermal Properties of the Cured Products

Thermal properties of the cured epoxy thermosets were investigated by DSC and TGA measurements and the results are

Table II. Thermal Properties of PSiN and Epoxy Thermosets

	In nitrogen		In air		
Samples	$T_{5\%}$ [a](°C)	Char (% at 750°C)	$T_{5\%}$ (°C)	T_{max} [b](°C)	Char (% at 750°C)
PsiN	313	4.3	313	-	1.3
CNE/PN	390	22.8	399	575	0.3
CNE/PN-10	388	34.3	399	604	9.0
CNE/PN-20	376	33.5	396	616	14.8

[a] $T_{5\%}$, 5% weight loss temperature.
[b] T_{max} temperature at the peak of the derivative thermogravimetric plots in the second degradation stage.

shown in Figures 8 and 9 and Table II. For comparison, the thermal decomposition behavior of PSiN was also studied. Figure 8 depicts the DSC plots of epoxy thermosets. Apparently, T_g of the epoxy thermosets decreases slightly with increasing PSiN loadings. For instance, the T_g value of CNE/PN is 161°C, which is 12°C and 18°C higher than those of CNE/PN-10 and CNE/PN-20, respectively. The slight reduction of T_g is mainly due to the decrease of the crosslinking density caused by the incorporation of PSiN. Moreover, the small-molecular-weight PSiN might play a role of "plasticizer" in the blended epoxy systems, which could also decrease the T_g of the systems.[12,13] The thermal stability and degradation behaviors of PSiN and cured epoxy thermosets were investigated by TGA measurements.

Figure 9 shows the TGA plots of weight retention versus temperature from 50 to 750°C in nitrogen and in air, respectively. The results are summarized in Table II. It can be seen that pure PSiN exhibits good thermal stability up to 300°C, after that it starts decomposing and has completely decomposed at around 400°C. CNE/PN shows higher thermal stability than PSiN and maintains most of their weights during heating up to 400°C both in nitrogen and in air. It is obvious that pure PSiN is less thermally stable than the CNE/PN resin. So the 5% weight loss temperature ($T_{5\%}$) of the cured resins decreases slightly with increasing PSiN contents. But the two epoxy samples containing PSiN can maintain most of their weights at 400°C both in nitrogen and in air, illustrating that the incorporation of PSiN hardly ruins the thermal stability of CNE/PN. Moreover, with the incorporation of PSiN, the char yields of CNE/PN blends with PSiN are higher than both PSiN and CNE/PN without PSiN. So we can infer the existence of reactions between the decomposition products of PSiN and CNE/PN. First decomposed P-containing groups might combine with crosslinked CNE/PN structures to afford high char yields.[15]

Furthermore, it is obviously observed that the epoxy thermosets exhibit different thermal decomposition behaviors in nitrogen and in air, respectively. According to the TGA plots, a sing-stage decomposition process is observed for the epoxy thermosets in nitrogen [Figure 9(a)]; however, a two-stage one is found in air environment [Figure 9(b)]. The first stage occurred between 350 and 500°C is mainly attributed to the decomposition of epoxy network due to the oxidative attacks. Addition of PSiN has little effects on the degradation process in this stage. The second stage begins at around 500°C and is mainly because of the subsequent thermo-oxidative degradation of the char.[13,25] The effect of PSiN on the thermal degradation process of CNE/PN mainly reflects in this stage, which can be clearly read from derivative thermogravimetric curves. As shown in Figure 9(c), the rapid weight loss temperature

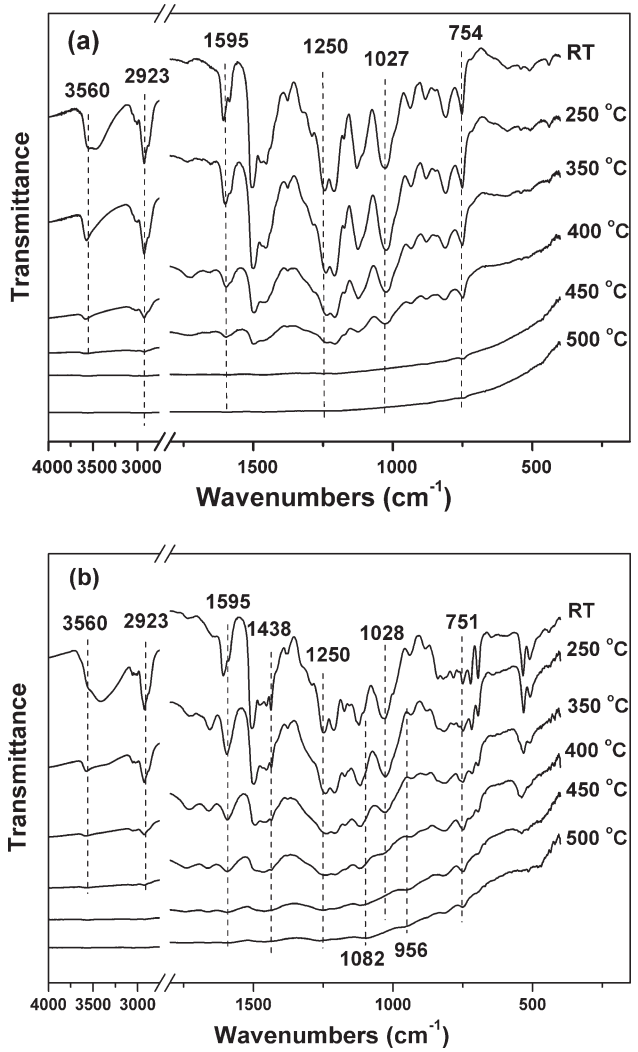

Figure 10. *In situ* FTIR spectra of epoxy thermoset. (a) CNE/PN; (b) CNE/PN-20.

Table III. Flame Retardant Properties of the Epoxy Thermosets

Samples	LOI (%)	pHRR[a] (kW m^{-2})	THR[b] (MJ m^{-2})	TTI[c] (s)	TTF[d] (s)	Burning time (s)	UL 94
CNE/PN	21	688	106	62	382	>30	Not V-2
CNE/PN-10	27.3	499	93	53	353	24.8	V-1
CNE/PN-20	32.2	438	85	48	281	9.5	V-0

[a] pHRR, peak of heat release rate.
[b] THR, total heat release.
[c] TTI, time to ignition.
[d] TTF, time to finish.

(T_{max}, determined with the peak of the DTG curves) in the second stage increases from 575°C (CNE/PN) to 616°C (CNE/PN-20). In other words, the resin with higher PSiN content is more stable at high temperature. Meanwhile, the residue char increases from 0.3 to 14.8% in air at 750°C with addition of 20 wt % PSiN. This phenomenon can be explained by the char yielding effect of PSiN. Both P-containing and Si-containing compounds can improve the char yielding ability of epoxy resins.[8,13,23,25–28] Higher char yield represents better flame retardancy, which is consistent with the UL 94 results presented later.

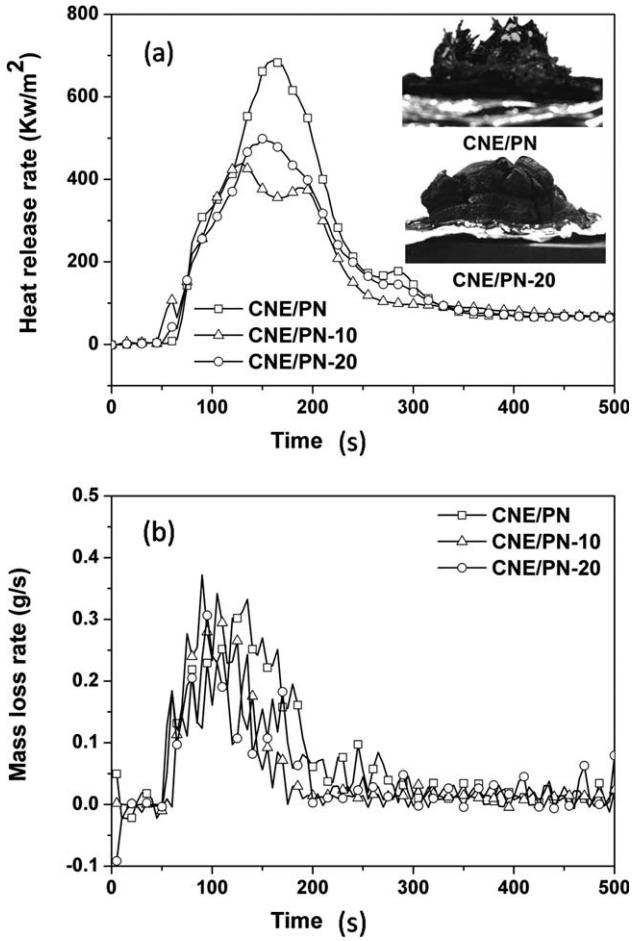

Figure 11. Heat release rates (a) and mass loss rates (b) of cured samples tested by cone calorimeter with 50 kW m^{-2}.

To further explore the char yielding effect of PSiN in air, the *in situ* FTIR was performed on the cured CNE/PN systems from room temperature to 500°C in air atmosphere. Figure 10 shows the *in situ* FTIR spectra of CNE/PN and CNE/PN-20 in air at various temperatures. For CNE/PN [Figure 10(a)], the absorption of hydroxyl group (—OH) at around 3560 cm^{-1} has gradually disappeared when the temperature increases from room temperature to 400°C.[9,29,30] Similarly, the absorptions of methyl ($—CH_3$) and methylene ($—CH_2—$) at around 2923 cm^{-1} also weaken little by little with the increasing of temperatures and disappear at temperatures over 400°C.[9,30] This process corresponds to the first decomposition stage in TGA testing. Similar results can be found in CNE/PN-20 system [Figure 10(b)]. Besides the characteristic absorptions of CNE/PN, peak at 1438 cm^{-1}, ascribed to PSiN, can be found in CNE/PN-20 system. For CNE/PN sample, almost all of the absorption peaks have disappeared at temperatures above 400°C except for the weak peaks at around 1595 and 754 cm^{-1}, which is attributed to the absorption of C═C and C—H in polyaromatic rings.[9,26,27] For CNE/PN-20 thermoset, not only the absorptions at 1595 and 751 cm^{-1}, but also peak at 1250 cm^{-1} still exist at 450°C. The absorption bands of 1250 and 1028 cm^{-1} are attributed to the structure of $C_6H_5—O—CH_2—$, which can be found both in CNE/PN and CNE/PN-20 thermosets.[9,29] When the temperature rises to 400°C, the two bands both disappear in CNE/PN. However, 1250 cm^{-1} band is preserved while 1028 cm^{-1} band disappeared in CNE/PN-20. This may be because the $C_6H_5—O—$ structure is retained, but turn to connect other groups instead of $–CH_2—$. At 500°C, all the organic components in CNE/PN have decomposed completely, whereas for the CNE/PN-20 thermoset, the new absorptions at 1082 cm^{-1} and 956 cm^{-1} arise. The former one is ascribed to the characteristic absorptions of Si—O bonds, indicating the formation of Si—O structure in the char. The other one represents the $Si—O—C_6H_5$ stretching vibrations, indicating that aromatic components are preserved in the char.[31]

All of these evidences suggest that the degradation process of epoxy resin has been retarded by the incorporation of PSiN, which promotes the formation of crosslinked char and thus slows down the weight loss rate at high temperature. This result is of great significance to the flame retardancy of CNE/PN.

Flame-retardant Properties

The percentage of oxygen in the O_2 and N_2 mixture, just sufficient to sustain the flame, is taken as the LOI. Table III summarizes the flame retardancy results of the cured epoxy resins.

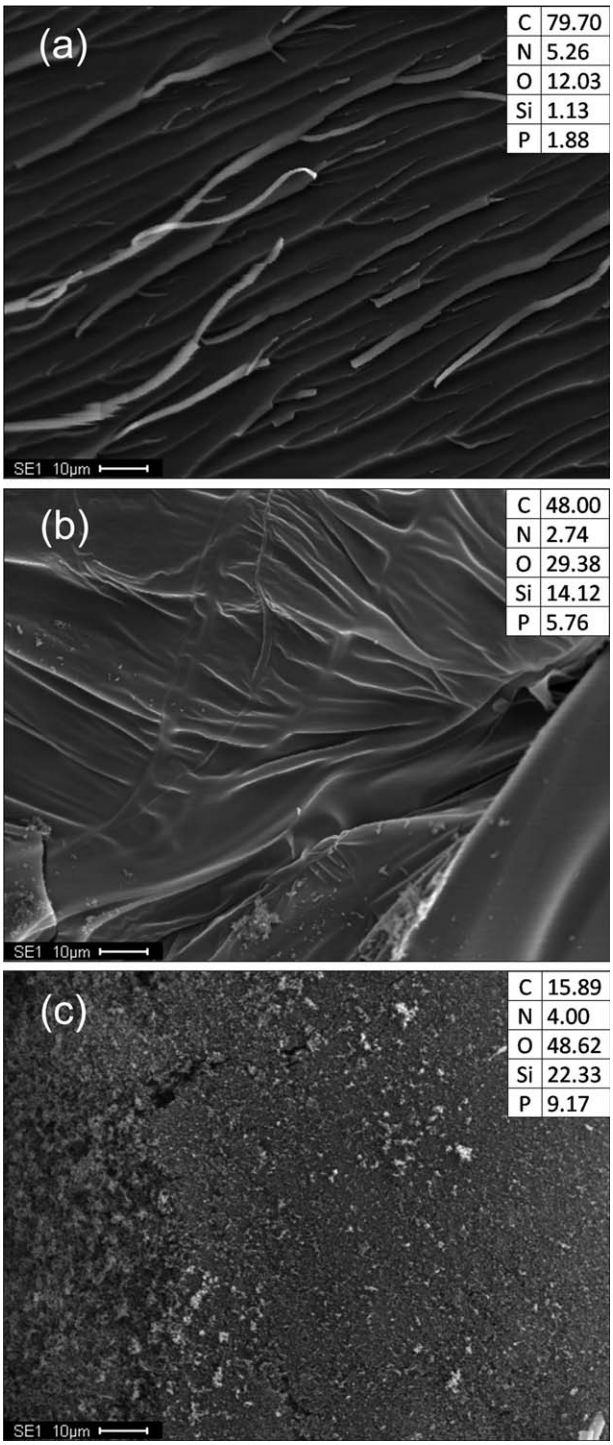

Figure 12. SEM graphs of CNE/PN-20 (a) before combustion; (b) inside of residue char after combustion; and (c) surface of residue char after combustion.

For CNE/PN, LOI value was only 21. With the addition of PSiN, the LOI increased to 27.3 and 32.2 for CNE/PN-10 and CNE/PN-20, respectively. The incorporation of PSiN results in a strong enhancement of LOI value, which might be attributed to the flame retardation effects of the three elements in PSiN.[8,20,23]

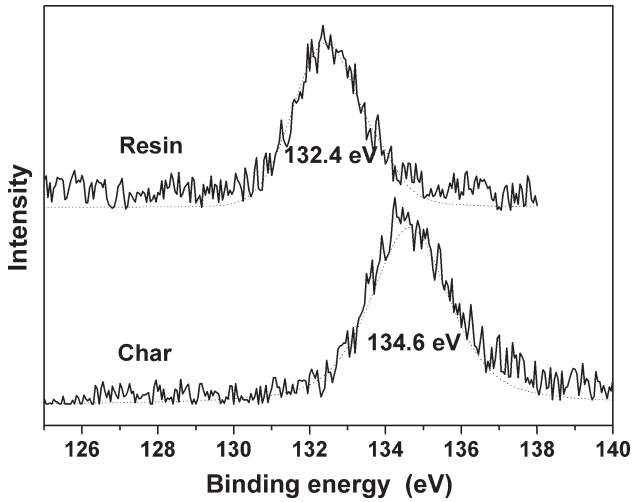

Figure 13. P2p XPS spectra of CNE/PN-20 before and after combustion.

The combustion behaviors of the cured epoxy resins were evaluated by cone calorimeter. Figure 11 displays the variation of heat releasing rates and mass loss rates with time. Both peak heat release rate (pHRR) and total heat release (THR) values of CNE/PN are greatly reduced by the addition of PSiN. For instance, the pHRR value of CNE/PN-20 is 438 kW m^{-2}, which is 36% lower than that of CNE/PN (688 kW m^{-2}). Time to ignition (TTI) of CNE/PN-20 is 48, lower than that of CNE/PN, which may be attributed to the poor thermal stability of PSiN. However, the time to finish (TTF) of CNE/PN-20 is lower than that of CNE/PN, obviously. In other words, the burning time of CNE/PN-20 (233 s) is much shorter than that of CNE/PN (320 s). Inside of Figure 11(a) shows the morphologies of residues after cone calorimeter. Compared with CNE/PN, CNE/PN-20 is more likely to form carbon foam layer after combustion. The incorporation of P-containing compounds is favorable for the formation carbon foam.[8] Moreover, *N*-containing compounds can boost the effect of P-containing compounds on the formation of carbon foam.[32]

The results above indicate that the incorporation of PSiN may make for the flame retardancy of the system. And this is further proved by the UL 94 testing. Even though suppressed burning dripping, the CNE/PN sample still meets no UL 94 rating due to long burning time. With 10 wt % of PSiN, CNE/PN-10 sample has UL 94 V-1 FR rating. Moreover, CNE/PN-20 sample can achieve UL 94 V-0 FR rating. All the results above demonstrate that the addition of PSiN to the CNE/PN can improve its flame retardancy. The flame-retardant mechanism will be discussed in the following section.

In order to discuss the FR mechanism of PSiN in CNE/PN, the residue char after cone calorimeter was studied. The morphologies of CNE/PN-20 sample before and after combustion were further investigated by SEM. Figure 12 displays the morphologies of CNE/PN-20 before combustion, the inside and surface of residue char, respectively. Moreover, the elementary contents of resin and the residue char were detected by EDX, and the data were listed in the SEM graphs. Although these data cannot represent the element contents exactly, they can be used to compare the element

contents of CNE/PN-20 before and after combustion.[32] From the results we can find that P, Si, and N present different variation trends. N content decreases because of its gasification, and it may play a part in gas phase FR.[20,32] Both P and Si contents increase sharply after combustion. This demonstrates that they could concentrate in the condense phase and play a role in FR.[8,13,23,25,31] Beside, P content was close to Si content before combustion. However, P content became lower than Si content after combustion. Therefore, we can infer that P may also take part in gas phase FR. Similar results could be found in Braun's work, which proposed that the release of phosphorus-containing volatiles increased with decreasing oxidation state of phosphorus.[9] To figure out the products of phosphorus compounds in the residue char after combustion, CNE/PN-20 resin before and after combustion were investigated by XPS, and the results are showed in Figure 13. The binding energy values of phosphorus in the CNE/PN-20 changed from 132.4 eV to 134.6 eV after combustion, indicating that the oxidation state of phosphorus had increased. Polyaromatic containing phosphate or pyrophosphate might be formed after combustion, which could play an important role in flame retardation.[30,32] Furthermore, all P, Si, and O contents in the surface of residue char are higher than that of inside, evidently. This phenomenon can mainly be attributed to two aspects. First, the epoxy samples lost much more carbon components in the surface segment than that of inside segment. Thus, the proportion of other elements, including O, P, and Si increased. Secondly, in the case of Si-containing flame retarding polymer systems, SiO_2 usually tends to migrate to surface because of its low surface energy.[23] Besides, char with high phosphorus contents shows better stability in combustion. So the surface char has higher phosphorus contents than inside so as to play a part in flame retardation.[8] Both P and Si element must exist combined with O, so all P, Si, and O contents in the surface of residue char are higher than that of inside. This surface char residue, which is rich in P and Si compounds, is important to the flame retardancy of polymers.

CONCLUSIONS

A novel phosphorous-silicone-nitrogen ternary FR, PSiN, was synthesized and applied in the flame retardancy of CNE/PN epoxy system. Flowability of the CNE/PN systems was improved by the addition of PSiN, but the T_g values of the epoxy thermosets decreased slightly with the increasing of PSiN loadings. Furthermore, the incorporation of PSiN was in favor of the thermal stability of epoxy thermosets, which might be attributed to the char yielding effects of P-containing and Si-containing components in PSiN. *In situ* FTIR results demonstrated that more char was preserved in CNE/PN-20 thermoset than that in CNE/PN during the thermal degradation process. LOI values of the epoxy system increased with the PSiN contents, while heat release value was reduced. An UL 94 V-0 rating was achieved when the weight contents of PSiN in the epoxy composites reached 20 wt %. Characterization of the residue char implied that silica tended to migrate to the surface of polymer for its low surface energy. Nitrogen components turned into gas in the combustion process. Phosphorus components played a role of FR in both condensed phase and gas phase. All the results indicated that current P-Si-N ternary FR might be a good candidate for epoxy flame retardancy.

ACKNOWLEDGMENTS

Financial support from the National Natural Science Foundation of China (51173188) is gratefully acknowledged.

REFERENCES

1. Delman, A. D. *J. Macromol. Sci. Part C: Rev. Macromol. Chem.* **1969**, *C3*, 281.
2. Laoutid, F.; Bonnaud, L.; Alexandre, M.; Lopez-Cuesta, J. M.; Dubois, P. *Mater. Sci. Eng. R-Rep.* **2009**, *63*, 100.
3. Lee, H.; Neville, K. Handbook of Epoxy Resins; McGraw-Hill: New York, **1972**.
4. Kinjo, N.; Ogata, M.; Nishi, K.; Kaneda, A. *Adv. Polym. Sci.* **1989**, *88*, 1.
5. Akatsuka, M.; Takezawa, Y.; Amagi, S. *Polymer* **2001**, *42*, 3003.
6. D'Silva, K.; Fernandes, A.; Rose, M. *Crit. Rev. Environ. Sci. Technol.* **2004**, *34*, 141.
7. Rakotomalala, M.; Wagner, S.; Döring, M. *Materials* **2010**, *3*, 4300.
8. Levchik, S. V. *J. Fire Sci.* **2006**, *24*, 345.
9. Braun, U.; Balabanovich, A. I.; Schartel, B.; Knoll, U.; Artner, J.; Ciesielski, M.; Döring, M.; Perez, R.; Sandler, J. K.; Altstädt, V. *Polymer* **2006**, *47*, 8495.
10. Liu, Y.-L.; Chang, G.-P.; Wu, C.-S. *J. Appl. Polym. Sci.* **2006**, *102*, 1071.
11. Zhang, X.-H.; Liu, F.; Chen, S.; Qi, G.-R. *J. Appl. Polym. Sci.* **2007**, *106*, 2391.
12. Ciesielski, M.; Schäfer, A.; Döring, M. *Polym. Adv. Technol.* **2008**, *19*, 507.
13. Ding, J.; Tao, Z.; Zuo, X.; Fan, L.; Yang, S. *Polym. Bull.* **2009**, *62*, 829.
14. Xiong, Y.-Q.; Zhang, X.-Y.; Liu, J.; Li, M.-M.; Guo, F.; Xia, X.-N.; Xu, W.-J. *J. Appl. Polym. Sci.* **2012**, *125*, 1219.
15. Shieh, J.-Y.; Wang, C.-S. *J. Polym. Sci. Part A: Polym. Chem.* **2002**, *40*, 369.
16. Perez, R. M.; Sandler, J. K. W.; Altstädt, V.; Hoffmann, T.; Pospiech, D.; Artner, J.; Ciesielski, M.; Döring, M.; Balabanovich, A. I.; Knoll, U.; Braun, U.; Schartel, B. *J. Appl. Polym. Sci.* **2007**, *105*, 2744.
17. Spontón, M.; Ronda, J. C.; Galià, M.; Cádiz, V. *J. Polym. Sci. Part A: Polym. Chem.* **2007**, *45*, 2142.
18. Song, T.; Li, Z. S.; Liu, J. G.; Yang, S. Y. *Chin. Chem. Lett.* **2012**, *23*, 793.
19. Horacek, H.; Grabner, W. *Makromol. Chem. Macromol. Symp.* **1993**, *74*, 271.
20. Horacek, H.; Grabner, R. *Polym. Degrad. Stab.* **1996**, *54*, 205.
21. Wang, W.; Perng, L.; Hsiue, G.; Chang, F. *Polymer* **2000**, *41*, 6113.
22. Mercado, L. A.; Galià, M.; Reina, J. A. *Polym. Degrad. Stab.* **2006**, *91*, 2588.

23. Hamdani, S.; Longuet, C.; Perrin, D.; Lopez-Cuesta, J.-M.; Ganachaud, F. *Polym. Degrad. Stab.* **2009**, *94*, 465.
24. Rey, P.; Taillades, J.; Rossi, J. C.; Gros, G. *Tetrahedron Lett.* **2003**, *44*, 6169.
25. Zhang, W.; Li, X.; Fan, H.; Yang, R. *Polym. Degrad. Stab.* **2012**, *97*, 2241.
26. Perret, B.; Schartel, B.; Stöß, K.; Ciesielski, M.; Diederichs, J.; Döring, M.; Krämer, J.; Altstädt, V. *Eur. Polym. J.* **2011**, *47*, 1081.
27. Qian, L.; Ye, L.; Qiu, Y.; Qu, S. *Polymer* **2011**, *52*, 5486.
28. Lin, L. K.; Wu, C. S.; Su, W. C.; Liu, Y. L. *J. Polym. Sci. Part A: Polym. Chem.* **2013**, *51*, 3523.
29. Wang, H.; Wang, Q.; Huang, Z.; Shi, W. *Polym. Degrad. Stab.* **2007**, *92*, 1788.
30. Wang, X.; Hu, Y.; Song, L.; Xing, W.; Lu, H.; Lv, P.; Jie, G. *Polymer* **2010**, *51*, 2435.
31. Zhang, W.; Li, X.; Li, L.; Yang, R. *Polym. Degrad. Stab.* **2012**, *97*, 1041.
32. Ma, H.; Fang, Z. *Thermochim. Acta* **2012**, *543*, 130.